



HAL
open science

Multi T1-weighted contrast MRI with fluid and white matter suppression at 1.5 T

Jérémy Beaumont, Hervé Saint-Jalmes, Oscar Acosta, Tobias Kober, Mark Tanner, Jean-Christophe Ferré, Olivier Salvado, Jürgen Fripp, Giulio Gambarota

► **To cite this version:**

Jérémy Beaumont, Hervé Saint-Jalmes, Oscar Acosta, Tobias Kober, Mark Tanner, et al.. Multi T1-weighted contrast MRI with fluid and white matter suppression at 1.5 T. *Magnetic Resonance Imaging*, 2019, 63, pp.217-225. 10.1016/j.mri.2019.08.010 . hal-02281467

HAL Id: hal-02281467

<https://univ-rennes.hal.science/hal-02281467v1>

Submitted on 20 Dec 2021

HAL is a multi-disciplinary open access archive for the deposit and dissemination of scientific research documents, whether they are published or not. The documents may come from teaching and research institutions in France or abroad, or from public or private research centers.

L'archive ouverte pluridisciplinaire **HAL**, est destinée au dépôt et à la diffusion de documents scientifiques de niveau recherche, publiés ou non, émanant des établissements d'enseignement et de recherche français ou étrangers, des laboratoires publics ou privés.



Distributed under a Creative Commons Attribution - NonCommercial 4.0 International License

MULTI T1-WEIGHTED CONTRAST MRI WITH FLUID AND WHITE MATTER SUPPRESSION AT 1.5T

J. Beaumont, MS^{1,2}, H. Saint-Jalmes, PhD¹, O. Acosta, PhD¹, T. Kober, PhD^{3,4,5}, M.

Tanner, BSc⁶, J.C. Ferré, MD, PhD^{7,8},

O. Salvado, PhD⁹, J. Fripp, PhD², G. Gambarota, PhD¹

1. Univ Rennes, CLCC Eugène Marquis, Inserm, LTSI-UMR1099, F-35000 Rennes, France
2. CSIRO, the Australian eHealth Research Centre, Herston, Queensland, Australia
3. Advanced Clinical Imaging Technology, Siemens Healthcare AG, Lausanne, Switzerland
4. Department of Radiology, University Hospital (CHUV), Lausanne, Switzerland
5. LTS5, Ecole Polytechnique Fédérale de Lausanne (EPFL), Lausanne, Switzerland
6. Invicro, A Konica Minolta Company, London, UK
7. Univ Rennes, Inria, CNRS, INSERM, IRISA, VISAGES ERL U-1228, F-35000 Rennes, France
8. CHU Rennes, Department of Neuroradiology, F-35033 Rennes, France
9. CSIRO, Data61, Herston, Queensland, Australia

Corresponding author: J. Beaumont; Mail address: Campus de Beaulieu, Université de Rennes
1, 35042 Rennes; Phone number: +33 633.905.869; Email: jeremy.beaumont.2@gmail.com

Acknowledgments

The authors thank the “Region Bretagne” which funded partially the work presented in the current study. The authors also thank the radiographers of Rennes University Hospital (Hôpital Sud) for their kind support. The volunteers were included in the OSS-IRM study, supported by the University Hospital of Rennes and the University of Rennes.

Running title: MULTI T1-WEIGHTED CONTRAST MRI AT 1.5T

MULTI T1-WEIGHTED CONTRAST MRI WITH FLUID AND WHITE MATTER SUPPRESSION AT 1.5T

Abstract

Introduction

The fluid and white matter suppression sequence (FLAWS) provides two T1-weighted co-registered datasets: a white matter (WM) suppressed contrast (*FLAWS1*) and a cerebrospinal fluid (CSF) suppressed contrast (*FLAWS2*). FLAWS has the potential to improve the contrast of the subcortical brain regions that are important for Deep Brain Stimulation surgery planning. However, to date FLAWS has not been optimized for 1.5T.

In this study, the FLAWS sequence was optimized for use at 1.5T. In addition, the contrast-enhancement properties of FLAWS image combinations were investigated using two voxel-wise FLAWS combined images: the division (*FLAWS-div*) and the high contrast (*FLAWS-hc*) image.

Methods

FLAWS sequence parameters were optimized for 1.5T imaging using an approach based on the use of a profit function under constraints for brain tissue signal and contrast maximization. MR experiments were performed on eleven healthy volunteers (age 18-30). Contrast (CN) and contrast to noise ratio (CNR) between brain tissues were measured in each volunteer. Furthermore, a qualitative assessment was performed to ensure that the separation between the internal globus pallidus (GPi) and the external globus pallidus (GPe) is identifiable in *FLAWS1*.

Results

The optimized set of sequence parameters for FLAWS at 1.5T provided contrasts similar to those obtained in a previous study at 3T. The separation between the GPi and the GPe was clearly

identified in *FLAWS1*. The CN of *FLAWS-hc* was higher than that of *FLAWS1* and *FLAWS2*, but was not different from the CN of *FLAWS-div*. The CNR of *FLAWS-hc* was higher than that of *FLAWS-div*.

Conclusion

Both qualitative and quantitative assessments validated the optimization of the FLAWS sequence at 1.5T. Quantitative assessments also showed that *FLAWS-hc* provides an enhanced contrast compared to *FLAWS1* and *FLAWS2*, with a higher CNR than *FLAWS-div*.

Keywords: brain, MRI, FLAWS, globus pallidus, image combination.

Introduction

The acquisition of magnetic resonance (MR) images with different contrasts (T1, T2, diffusion, ...) is today a standard procedure in both research and clinical practice. Typically, images are acquired in separate measurements and then pre-processing steps -such as co-registration- are needed to spatially normalize the data before analysis. In this context, magnetic resonance imaging (MRI) sequences that provide, in a single acquisition, co-registered datasets with different contrasts are of interest to reduce the amount of data processing and to minimize loss of information due to interpolation and other possible confounding effects.

The **fluid and white matter suppression (FLAWS)** sequence [1], derived from the **magnetization-prepared two rapid gradient-echoes (MP2RAGE)** sequence [2], was introduced to provide two co-registered T1-weighted images of the brain with different contrasts in a single acquisition. The first contrast (*FLAWS1*) is characterized by the suppression of the white matter (WM) signal, yielding an image with a contrast similar to the one provided by the **fast gray matter acquisition T1 inversion recovery (FGATIR)** sequence [3]. The WM-suppressed contrast can be used to improve the visualization of basal ganglia structures such as the globus pallidus [4–6] and to detect epileptogenic lesions in focal cortical dysplasia [7]. The second contrast (*FLAWS2*) is similar to the contrast obtained with the **magnetization-prepared rapid gradient-echo (MPRAGE)** sequence [8]. This contrast is considered as being the standard T1-weighted anatomical contrast of the brain, with a suppression of the cerebrospinal fluid (CSF) signal.

A recent study performed at 3T showed that FLAWS imaging allows for a good visualization of basal ganglia structures and facilitates **deep brain stimulation (DBS)** surgery planning [6]. However, most of the centers performing DBS employ 1.5T MR systems [9,10]. These centers

would benefit from the use of FLAWS for surgery planning, but to the best of our knowledge there is no study reporting the optimization of FLAWS imaging at 1.5T.

The co-registration properties of the MP2RAGE and FLAWS images allow to perform voxel-wise operations for generating new sets of images characterized by new T1 contrasts. Van de Moortele et al. [11] and Marques et al. [2] investigated the properties of the voxel-wise division of MP2RAGE images. They determined that the result of this image combination was free of signal variations induced by the received bias field (B_1^-), proton density (M_0) and $T2^*$. Division images were also used by Bannier et al. [6] in the case of FLAWS, but the signal properties of the FLAWS division image were not investigated. Another image combination was proposed by Tanner et al. [1] to provide a gray matter specific contrast by computing the voxel-wise minimum of FLAWS images. [FLAWS image combinations were also used by Wang et al. to develop a fast brain tissue segmentation method \[12\].](#)

In this context, the aim of the current study was twofold. The first aim was to determine the optimal sequence parameters of FLAWS for 1.5T MR imaging. Given the complexity and the multi-parametric nature of this sequence optimization, an approach based on the use of a profit function was employed. The second aim of this study was to investigate the properties of FLAWS voxel-wise division images and to propose an improved approach for combining FLAWS images for tissue contrast enhancement.

Materials and methods

1.1. Sequence optimization

The goal of this optimization was to obtain FLAWS images at 1.5T with a contrast similar to that obtained at 3T by Tanner et al. [1], that is, a WM-suppressed contrast in *FLAWSI* and a CSF-

suppressed contrast in *FLAWS2*. The quality of the optimization was assessed using the standard definition of the contrast (CN) and contrast-to-noise ratio (CNR) [1].

The signal of *FLAWS1* and *FLAWS2* depends on the following set of sequence parameters (Φ):

$$\Phi = [\alpha_1, \alpha_2, TI_1, TI_2, TR_{GRE}, TR_{Seq}, N_{Ex}] \quad 1.$$

where α_1 and α_2 are the flip angles of the Gradient Echo (GRE) modules, acquired at two different inversion times, TI_1 and TI_2 , TR_{GRE} is the repetition time of the GRE modules, TR_{Seq} is the sequence repetition time, corresponding to the time interval between two consecutive inversion pulses and N_{Ex} is the number of excitations per GRE module. We define as Φ_{opt} the set of parameters which provides the optimal contrasts for FLAWS at 1.5T, i.e. contrasts similar to those obtained at 3T by Tanner et al. [1].

Given the complexity and the multi-parametric nature of the FLAWS signal, we proposed a novel strategy for the optimization of the FLAWS sequence. The optimization was performed in two steps. In the first step, an approach based on the use of a profit function was employed to determine pre-optimal parameter sets. In the second step, the optimal set was selected among the pre-optimal sets by maximizing the contrast between brain tissues.

In the following formulae, we will use the subscripts W , G , GP and C to denote white matter, grey matter, the globus pallidus and cerebrospinal fluid, respectively.

Profit function

The profit function P was defined to: (1) suppress the WM signal in *FLAWS1* ($S1_W$) while facilitating the visualization of the globus pallidus -this is accomplished by increasing the profit when $(S1_{GP} - S1_W)$ increases; (2) suppress the CSF signal in *FLAWS2* ($S2_C$) by decreasing the profit when $S2_C$ increases; (3) maximize the CNR between brain tissues by increasing the profit

when the sum $S1_G + S1_C + S2_W + S2_G$ is increasing. Based on the aforementioned criteria, the profit function P was written as:

$$P_m^k(\Phi) = k(S1_{GP}(\Phi) - S1_W(\Phi)) - m S2_C(\Phi) + S1_G(\Phi) + S1_C(\Phi) + S2_W(\Phi) + S2_G(\Phi) \quad 2.$$

where k and m are regularization parameters allowing to adjust the importance of the globus pallidus visualization and WM and CSF suppression in the optimization.

Profits were computed for every pair of regularization parameters (k, m) , with both k and m varying between 0 and 100 (step-size: 1). Each couple (k, m) is associated to a pre-optimal set of parameters $\Phi_{opt}^{k,m}$ which maximize the profit $P_m^k(\Phi)$.

Contrast maximization

Among all the pre-optimal parameter sets $\Phi_{opt}^{k,m}$, the optimal parameter set Φ_{opt} was defined as the one maximizing the sum of the simulated contrast between the tissues ($\sum CN = CN1_{W/G} + CN1_{W/C} + CN1_{G/C} + CN2_{W/G} + CN2_{W/C} + CN2_{G/C}$).

Signal simulations

The signal of *FLAWS1* and *FLAWS2* was simulated using the Bloch equations, implemented in *Mathematica* (Wolfram Research, Inc, Champaign, IL, USA). Signal simulations were performed using 1.5T tissue properties reported in the literature [13–15]: T1 relaxation times were fixed to 0.65 sec for WM, 0.75 sec for the globus pallidus, 1.2 sec for GM and 4 sec for CSF; proton densities of WM, the globus pallidus, GM and CSF were respectively fixed to 0.7, 0.72, 0.8 and 1.

Based on preliminary MRI experiments, a voxel size of $1.25 \times 1.25 \times 1.4 \text{ mm}^3$ was considered to be the best compromise between SNR maximization and spatial resolution within a maximum acquisition time of 10 minutes. Consequently, the number of slices (N_{slices}) was set to 128 and the matrix size was set to 180×192 to obtain a spatial coverage sufficiently large to avoid

artefacts due to aliasing. The slice partial Fourier was set to 6/8 to allow the acquisition of FLAWS images with WM signal suppression [1]. According to the size of the matrix and the constraints on the acquisition time, the maximum sequence repetition time should not exceed 3.5 sec.

The optimization was performed on a wide range of parameter combinations, with α_1 and α_2 ranging from 3° to 13° (step-size 1°); TI_1 ranging from 0.37 sec to 1.41 sec (step-size 0.02 sec); TI_2 ranging from 1 sec to 3.2 sec (step-size 0.02 sec); TR_{GRE} equals to 4.16 msec; TR_{Seq} ranging from 2.5 sec to 3.5 sec (step-size 0.1 sec); N_{Ex} equals to $6/8 * N_{Slices}$. With this choice of parameter combinations, we obtained 9×10^6 parameter sets Φ . Out of this pool, we selected 4×10^4 parameter sets Φ that provided the typical contrasts of the FLAWS, ie. WM suppression in *FLAWS1* and CSF suppression in *FLAWS2*. From these 4×10^4 combinations, 10^4 pre-optimal parameter sets $\Phi_{opt}^{k,m}$ were determined using the profit function. Among these parameter sets $\Phi_{opt}^{k,m}$, the optimal parameter set Φ_{opt} was defined as the one maximizing the sum of the contrast $\sum CN$ between brain tissues.

1.2. Voxel-wise image combination

Voxel-wise image combinations of *FLAWS1* and *FLAWS2* were investigated to enhance the contrast between brain tissues. The metrics used to analytically compare different types of combinations were the contrast (CN) and the signal to noise ratio (SNR).

First, the properties of the FLAWS division image (*FLAWS-div*) were investigated. Then, a FLAWS-dedicated image-combination, denoted here as FLAWS high contrast image (*FLAWS-hc*), was proposed.

For sake of clarity, mathematical demonstrations associated to the work presented in the following sections are provided in supplementary materials.

Properties of the division image (FLAWS-div)

FLAWS-div is computed using the voxel-wise operation:

$$S_{div_A} = \frac{S1_A}{S2_A} \quad 3.$$

where $S1_A$ ($S2_A$) is the signal of a given tissue A in *FLAWS1* (*FLAWS2*). It can be shown that the WM/GM, WM/CSF and GM/CSF contrasts are close to 1 in the division image (see supplementary materials). Additionally, mathematical demonstrations show that the SNR of WM and CSF is low in *FLAWS-div*.

Properties of the high contrast image (FLAWS-hc)

The high contrast image, *FLAWS-hc*, is obtained by computing the voxel-wise signed contrast between *FLAWS1* and *FLAWS2*:

$$Shc_A = \frac{S1_A - S2_A}{S1_A + S2_A} \quad 4.$$

Therefore, *FLAWS-hc* values are included within the [-1,1] interval. It should be noted that *FLAWS-hc* is free of signal variations due to the received bias field, T2* relaxation and proton density [2].

It can be shown that the WM/CSF contrast is close to 1 in *FLAWS-hc*. In addition, either the WM/GM contrast or the GM/CSF contrast tends towards 1, according to the sign of $(S1_G - S2_G)$ (see supplementary materials). Mathematical demonstrations showed that the SNR of WM and CSF is higher in *FLAWS-hc* than in *FLAWS-div*.

Similarly to the *FLAWS-div* and the MP2RAGE-dedicated combination image [2,11], *FLAWS-hc* is characterized by the appearance of a salt and pepper noise in its background. This noise can be removed by adding coefficients in the voxel-wise operations [16]. A preliminary investigation on

the high-contrast image was recently proposed for presentation at a conference [17] using a dataset of FLAWS images that, however, were not fully optimized.

1.3. MRI experiments and data analysis

To assess the results of the optimization, MR imaging was performed on [eleven healthy volunteers \(four females, age 18-30yo\)](#) with a 1.5T scanner (MAGNETOM Aera, Siemens Healthcare, Erlangen, Germany) equipped with a 20-receiver channel head and neck matrix coil, using the optimal parameter set Φ_{opt} . [MR acquisitions were performed without parallel imaging for all the volunteers and with parallel imaging \(2x GRAPPA acceleration\) on a subset of four volunteers.](#) All experiments were approved by the Institutional Review Board and the volunteers signed an informed consent form to be included in the study.

To compare the results of the current study with those obtained at 3T by Tanner et al. [1], the CN and CNR between brain tissues were measured in regions of interests (ROI) manually drawn in the corpus callosum (splenium) for WM, caudate nucleus (head) for GM and lateral ventricle for CSF. The size of the ROI was 46 mm^3 for each tissue, across all datasets. A qualitative assessment of the acquired images was performed to ensure that the separation between the internal globus pallidus (GPi) and the external globus pallidus (GPe) was identifiable in *FLAWS1*.

Results

The sum of the six simulated contrast ($\sum CN$), computed for each pre-optimal parameter set $\Phi_{opt}^{k,m}$, is illustrated in Figure 1. In this figure, we observe different plateaus, that is, regions where multiple pairs (k, m) yield the same value of $\sum CN$. A low value of $\sum CN$ was observed within the plateau around $(k = 0, m = 0)$, illustrated in dark blue color. A high value of $\sum CN$ was found within the plateau illustrated in orange color, containing the pair $(k = 100, m = 100)$. The

maximum value of $\sum CN$ was found within the plateau illustrated in red color corresponding to the pair $(k = 44, m = 77)$. The associated set of parameters $(\Phi_{\text{opt}} = [\alpha_1, \alpha_2, TI_1, TI_2, TR_{GRE}, TR_{Seq}, N_{Ex}])$ is presented in Table 1.

Figure 2 shows the signal of *FLAWS1* and *FLAWS2* for pre-optimal sets of parameters associated to three different pairs of regularization parameters $(k, m: 0,0; 44,77; 100,100)$.

The signal corresponding to the pair $(k = 0, m = 0)$ is characterized by a poor WM suppression in *FLAWS1* (dashed blue line) and a poor CSF suppression in *FLAWS2* (continuous blue line). The pair $(k = 100, m = 100)$ yields WM and GM signals with a very low intensity in *FLAWS2* (continuous orange line).

As opposed to the case of the two pairs presented above, the signal of the pair $(k = 44, m = 77)$ does not suffer from the aforementioned disadvantages. On the contrary, this signal is characterized by a good WM suppression in *FLAWS1* (dashed red line) and a good CSF suppression in *FLAWS2* (continuous red line). Moreover, the signals of WM and GM in *FLAWS2* have a high intensity (continuous red line).

Figure 3 shows 1.5T FLAWS images acquired with the optimal set of parameters, corresponding to the pair $(k = 44, m = 77)$ and presented in Table 1. *FLAWS1* is characterized by an excellent WM suppression, as easily visualized on the sagittal view. An excellent CSF suppression was observed in *FLAWS2*. These images displayed a strong bias, as particularly evident in the sagittal views.

For every set of FLAWS images, the separation between the GPe and the GPi was identified in *FLAWS1*, whereas it could not be identified in *FLAWS2*, as shown in Figure 4.

Table 2 presents the simulated and *in-vivo* values of contrast obtained at 1.5T with the optimal set of parameters indicated in Table 1. Results obtained at 3T by Tanner et al. [1] are also reported.

The simulated contrast was consistent with the contrast measured *in-vivo* at 1.5T. A good agreement between the contrast reported at 1.5T and 3T was also found.

Figure 5 shows the image combinations *FLAWS-div* and *FLAWS-hc*. These images display an excellent WM suppression, similarly to *FLAWS1*. Furthermore, *FLAWS-div* and *FLAWS-hc* are also characterized by a high signal intensity of the CSF. Figure 6 highlights the contrast enhancement provided by *FLAWS-hc* compared to *FLAWS1*. For example, the enhanced GM/CSF contrast provides a clear separation between the cerebellum and the CSF. This separation is not identifiable in *FLAWS1*. Furthermore, *FLAWS-hc* provides an image with reduced bias compared to *FLAWS1*. This is noticeable when comparing the CSF signal in the cortical regions to the CSF signal nearby the cerebellum. Contrast-enhanced images with a contrast similar to *FLAWS2* can be obtained by computing the opposite of *FLAWS-hc* (*FLAWS-hco*), that is, multiplying *FLAWS-hc* by -1 . As observed in *FLAWS-hc*, *FLAWS-hco* displays a contrast enhancement and a bias field reduction.

Table 3 presents the CN and CNR of *FLAWS1*, *FLAWS2*, *FLAWS-div* and *FLAWS-hc*. The minimum total CN of *FLAWS-div* is higher than the maximum total CN of *FLAWS1* and *FLAWS2*. The minimum total CN of *FLAWS-hc* is also higher than the maximum total CN of *FLAWS1* and *FLAWS2*. The total CN of *FLAWS-hc* is not different from the total CN of *FLAWS-div*. However, the minimum total CNR of *FLAWS-hc* is higher than the maximum total CNR of *FLAWS-div*. *FLAWS-hc* is also characterized by a higher total CNR than *FLAWS1*. No difference was found between the total CNR of *FLAWS2* and *FLAWS-hc*.

FLAWS images acquired with parallel imaging are characterized by a contrast similar to the one obtained without parallel imaging, as presented in Figure 7 and Supplementary Table 1. Supplementary Table 1 shows that the CNR between brain tissues remains high in parallel FLAWS images. However, the CNR provided by the parallel imaging FLAWS was slightly

lower than the CNR of the standard FLAWS. This decrease in CNR hampered the visualization of basal ganglia structures in parallel imaging FLAWS images, as shown in Supplementary Figure 1.

An incidental finding (periventricular GM heterotopia) was found in one of the volunteers. The contrast enhancement provided by *FLAWS-hc* allowed to better identify the incidental finding compared to *FLAWS1* and *FLAWS2* (Figure 8). This incidental finding was also clearly identified in the FLAWS minimum image (*FLAWS-min*). FLAWS images acquired with parallel imaging also allowed to identify the periventricular GM heterotopia, as shown in Supplementary Figure 2.

Discussion

In this study, we optimized FLAWS imaging at the field strength of 1.5T. The optimization was carried out by performing signal simulations using the Bloch equations and applying a strategy that employs a profit function. FLAWS images were acquired *in vivo*, with the most favorable set of sequence parameters obtained by the optimization procedure. Qualitative and quantitative assessment of FLAWS images at 1.5T validated the optimization approach proposed in this study. Furthermore, the co-registration properties of *FLAWS1* and *FLAWS2* provided us the opportunity of investigating image combinations (*FLAWS-div* and *FLAWS-hc*).

The choice of a novel MRI optimization approach, relying on the use of a profit function, was driven by the multiparametric nature of the problem. As a matter of fact, the signal intensity in FLAWS depends on seven parameters $[\alpha_1, \alpha_2, T_{I_1}, T_{I_2}, TR_{GRE}, TR_{Seq}, N_{Ex}]$; moreover, the same set of parameters has to provide different targeted contrasts in two sets of images, *FLAWS1* and *FLAWS2*.

The optimization consisted of three steps: (i) the sequence parameters providing a simulated contrast similar to FLAWS at 3T were extracted from a wide range of sets; (ii) among the sets of

parameters extracted in step (i), pre-optimal sets were selected by maximizing a profit function aimed at tailoring the WM and CSF signal suppression in the optimization; and (iii) the optimal set was chosen from the pre-optimal sets to maximize the simulated contrast between brain tissues. To obtain *FLAWS1* images where the separation between the GPe and the GPi is identifiable, the profit function was designed to suppress the WM and, at the same time, to maximize the difference between the globus pallidus and WM.

The MRI experiments performed on healthy volunteers at 1.5T validated the results of our optimization procedure. An excellent WM and CSF signal suppression was observed in *FLAWS1* and *FLAWS2*, respectively. The values of the contrast measured *in-vivo* at 1.5T were consistent with the simulated values and with the values reported at 3T [1]. From a qualitative point of view, the optimal parameters of FLAWS at 1.5T allowed to identify the separation between the GPe and the GPi in *FLAWS1*. This could be of interest for DBS surgery planning at 1.5T, which is the field strength employed by most of the centers performing DBS [9,10].

In the current study, we investigated FLAWS-dedicated image combinations. First, the properties of the division image *FLAWS-div* were presented. It was shown, by theoretical arguments and quantitative measurements, that the contrast between brain tissues in *FLAWS-div* tends towards 1. A previous study investigated the use of FLAWS imaging, and specifically *FLAWS-div*, at 3T for DBS surgery planning. In this study, the authors exploited the enhanced contrast of *FLAWS-div* to visualize the basal ganglia. However, we showed in the current study that *FLAWS-div* is characterized by a poor SNR in both WM and CSF, leading to a low CNR between brain tissues. To overcome the CNR limitation of *FLAWS-div*, a new combination image, *FLAWS-hc*, was proposed. Mathematical demonstrations and quantitative measurements showed that *FLAWS-hc* is characterized by a high CN and CNR between brain tissues. Furthermore, *FLAWS-hc* has a contrast similar to *FLAWS1*, but provides a better differentiation of GM structures from the CSF

thanks to its contrast-enhancement properties. In addition, the incidental periventricular GM heterotopia observed in the FLAWS images of a volunteer highlights the interest of FLAWS for clinical applications. In particular, the contrast provided by the FLAWS combination images, *FLAWS-hc* and *FLAWS-min*, represents an added value in clinical settings.

FLAWS-hc images are characterized by a signal free of T2* relaxation, proton density and received bias field, similarly to the MP2RAGE combination image [2]. The comparison between *FLAWS1* and *FLAWS-hc* highlights the bias field reduction obtained in *FLAWS-hc*. The opposite of *FLAWS-hc* (*FLAWS-hco*) provides a CSF signal suppression, as the MPRAGE images and the MP2RAGE combination images. Like the MP2RAGE combination image, *FLAWS-hco* is free of T2* relaxation, proton density and received bias field and thus could be of interest for brain segmentation at ultra-high fields.

A previous study performed at 3T showed the relevance of FLAWS imaging for the detection of epileptogenic zones in focal-cortical dysplasia [7] and suggested that 7T FLAWS imaging might improve the detection of epileptogenic zones. Our investigation of the combination-images indicates that the contrast-enhancement and bias field reduction of *FLAWS-hc* provide an added value for FLAWS imaging at ultra-high fields. It should be noted that the transmitted-bias field affects the signal of *FLAWS-hc*. This aspect should be carefully taken into account for the optimization and implementation of FLAWS at ultra-high fields.

In the current study, in addition to the 10-min FLAWS protocol without parallel imaging, a 6-min protocol (*2x GRAPPA acceleration*) was tested. The shorter protocol yielded images of diagnostic quality similar to the long protocol, as highlighted by the unequivocal observation of the incidental finding. As such, the 6-min FLAWS protocol is of potential interest for diagnostic purposes; however, this protocol cannot be used for DBS surgery planning, where an accurate identification of the different basal-ganglia structures is required.

The current study has some limitations. First, MRI experiments were performed only on a small number of [young](#) volunteers. In future studies, it will be necessary to acquire data on a large cohort of patients, in order to assess the impact of FLAWS imaging on DBS surgery planning at 1.5T. Furthermore, as opposed to the division image *FLAWS-div*, the newly proposed combination image *FLAWS-hc* is not readily available on the MRI console, that is, is not yet reconstructed online on the user interface of the MR systems; as such, the combination image *FLAWS-hc* needs to be computed offline. [The FLAWS protocol proposed in the current study for DBS surgery planning takes 10 minutes. Compressed sensing techniques could be employed to decrease the protocol acquisition time. However, these techniques were not readily available on the clinical system used in the current study.](#)

In conclusion, we optimized FLAWS brain imaging at 1.5T for a potential application to DBS surgery planning. In addition, the co-registration properties of FLAWS images were exploited to generate the combination image *FLAWS-hc*, which is characterized by an enhanced contrast between brain tissues. With a signal free of T2* relaxation, proton density and received bias field, *FLAWS-hc* can be of interest for ultra-high field imaging.

Declarations of interest

Tobias Kober is employed by Siemens Healthcare, Switzerland.

References

- [1] Tanner M, Gambarota G, Kober T, Krueger G, Erritzoe D, Marques JP, et al. Fluid and white matter suppression with the MP2RAGE sequence. *J Magn Reson Imaging* 2012;35:1063–70. doi:10.1002/jmri.23532.
- [2] Marques JP, Kober T, Krueger G, van der Zwaag W, Van de Moortele P-F, Gruetter R. MP2RAGE, a self bias-field corrected sequence for improved segmentation and T1-mapping at high field. *Neuroimage* 2010;49:1271–81. doi:10.1016/j.neuroimage.2009.10.002.
- [3] Sudhyadhom A, Haq IU, Foote KD, Okun MS, Bova FJ. A high resolution and high contrast MRI for differentiation of subcortical structures for DBS targeting: The Fast Gray Matter Acquisition T1 Inversion Recovery (FGATIR). *Neuroimage* 2009;47:T44–52. doi:10.1016/j.neuroimage.2009.04.018.
- [4] Martin-Bastida A, Ward RJ, Newbould R, Piccini P, Sharp D, Kabba C, et al. Brain iron chelation by deferiprone in a phase 2 randomised double-blinded placebo controlled clinical trial in Parkinson's disease. *Sci Rep* 2017;7:1398. doi:10.1038/s41598-017-01402-2.
- [5] Niccolini F, Haider S, Reis Marques T, Muhlert N, Tziortzi AC, Searle GE, et al. Altered PDE10A expression detectable early before symptomatic onset in Huntington's disease. *Brain* 2015;138:3016–29. doi:10.1093/brain/awv214.
- [6] Bannier E, Gambarota G, Ferre J-C, Kober T, Nica A, Chabardes S, et al. FLAWS imaging improves depiction of the thalamic subregions for DBS planning in epileptic patients. *Int. Soc. Magn. Reson. Med.*, 2018.
- [7] Chen X, Qian T, Kober T, Zhang G, Ren Z, Yu T, et al. Gray-matter-specific MR imaging

- improves the detection of epileptogenic zones in focal cortical dysplasia: A new sequence called fluid and white matter suppression (FLAWS). *NeuroImage Clin* 2018;20:388–97. doi:10.1016/J.NICL.2018.08.010.
- [8] Mugler JP, Brookeman JR. Three-dimensional magnetization-prepared rapid gradient-echo imaging (3D MP RAGE). *Magn Reson Med* 1990;15:152–7.
- [9] Jiltsova E, Möttönen T, Fahlström M, Haapasalo J, Tähtinen T, Peltola J, et al. Imaging of Anterior Nucleus of Thalamus Using 1.5T MRI for Deep Brain Stimulation Targeting in Refractory Epilepsy. *Neuromodulation Technol Neural Interface* 2016;19:812–7. doi:10.1111/ner.12468.
- [10] Larson PS, Richardson RM, Starr PA, Martin AJ. Magnetic Resonance Imaging of Implanted Deep Brain Stimulators: Experience in a Large Series. *Stereotact Funct Neurosurg* 2008;86:92–100. doi:10.1159/000112430.
- [11] Van de Moortele P-F, Auerbach EJ, Olman C, Yacoub E, Uğurbil K, Moeller S. T1 weighted brain images at 7 Tesla unbiased for Proton Density, T2* contrast and RF coil receive B1 sensitivity with simultaneous vessel visualization. *Neuroimage* 2009;46:432–46. doi:10.1016/J.NEUROIMAGE.2009.02.009.
- [12] Wang Y, Wang Y, Zhang Z, Xiong Y, Zhang Q, Yuan C, et al. Segmentation of gray matter, white matter, and CSF with fluid and white matter suppression using MP2RAGE. *J Magn Reson Imaging* 2018. doi:10.1002/jmri.26014.
- [13] Wright PJ, Mouglin OE, Totman JJ, Peters AM, Brookes MJ, Coxon R, et al. Water proton T1 measurements in brain tissue at 7, 3, and 1.5T using IR-EPI, IR-TSE, and MPRAGE: results and optimization. *Magn Reson Mater Physics, Biol Med* 2008;21:121–30. doi:10.1007/s10334-008-0104-8.
- [14] Rooney WD, Johnson G, Li X, Cohen ER, Kim S-G, Ugurbil K, et al. Magnetic field and

- tissue dependencies of human brain longitudinal $^1\text{H}_2\text{O}$ relaxation in vivo. *Magn Reson Med* 2007;57:308–18. doi:10.1002/mrm.21122.
- [15] Vymazal J, Righini A, Brooks RA, Canesi M, Mariani C, Leonardi M, et al. T1 and T2 in the Brain of Healthy Subjects, Patients with Parkinson Disease, and Patients with Multiple System Atrophy: Relation to Iron Content. *Radiology* 1999;211:489–95. doi:10.1148/radiology.211.2.r99ma53489.
- [16] O'Brien KR, Kober T, Hagmann P, Maeder P, Marques J, Lazeyras F, et al. Robust T1-Weighted Structural Brain Imaging and Morphometry at 7T Using MP2RAGE 2014. doi:10.1371/journal.pone.0099676.
- [17] Beaumont J, Saint-Jalmes H, Acosta O, Kober T, Tanner M, Ferré J-C, et al. High Contrast T1-Weighted MRI with Fluid and White Matter Suppression Using MP2RAGE. *IEEE Int. Symp. Biomed. Imaging*, Venice, Italy: 2019.

Table 1: Optimal parameters of the FLAWS sequence at 1.5T.

TR/TE (msec)	3500/2.32
TI (msec)	403/1030
Flip angles	6°/10°
Matrix	180 × 192
Slices	128
Resolution (mm ³)	1.25 × 1.25 × 1.4
BW (Hz/px)	240
Orientation	<i>Sagittal</i>
FOV (mm ²)	225 × 240
GRAPPA	<i>None (or 2x acceleration)</i>
Slice partial Fourier	6/8
Scan time (min: sec)	10:27 (or 05:50)

Table 2: Simulated and in-vivo values of contrast at 1.5T in FLAWS1 and FLAWS2. For reference, the values obtained at 3T by Tanner et al. are also shown [1].

Contrast	FLAWS1			FLAWS2		
	Simulation 1.5T	<i>In-vivo</i> 1.5T	<i>In-vivo</i> 3T [1]	Simulation 1.5T	<i>In-vivo</i> 1.5T	<i>In-vivo</i> 3T [1]
WM/GM	0.88	0.69 (0.59-0.84)	0.59 (0.51-0.69)	0.29	0.23 (0.19-0.28)	0.15 (0.13-0.16)
WM/CSF	0.90	0.75 (0.67-0.89)	0.68 (0.62-0.77)	1.00	0.88 (0.82-0.93)	0.83 (0.68-0.89)
GM/CSF	0.09	0.12 (0.08-0.19)	0.16 (0.13-0.17)	0.99	0.81 (0.72-0.89)	0.78 (0.60-0.86)
Total*	1.87	1.56 (1.39-1.91)	-	2.28	1.92 (1.77-2.04)	-

WM: White Matter, GM: Gray Matter, CSF: Cerebrospinal Fluid. *In-vivo* contrast measurements were performed in the corpus callosum (splenium) for WM, caudate nucleus (head) for GM and lateral ventricle for CSF. Ranges of *in-vivo* contrasts are presented in parentheses.

*Total is the mean sum of the contrast WM/GM, WM/CSF and GM/CSF calculated for each volunteer.

Table 3: Average values of contrast (CN) and contrast to noise ratio (CNR) for the FLAWS sequence acquired with optimal parameters at 1.5T.

	<i>FLAWS1</i>	<i>FLAWS2</i>	<i>FLAWS-div</i>	<i>FLAWS-hc</i>
CN				
WM/GM	0.69 (0.59-0.84)	0.23 (0.19-0.28)	0.80 (0.73-0.89)	0.58 (0.48-0.64)
WM/CSF	0.75 (0.67-0.89)	0.88 (0.82-0.93)	0.98 (0.97-0.99)	1.00 (1.00-1.00)
GM/CSF	0.12 (0.08-0.19)	0.81 (0.72-0.89)	0.87 (0.77-0.93)	1.00 (1.00-1.00)
TotalCN*	1.56 (1.39-1.91)	1.92 (1.77-2.04)	2.65 (2.51-2.77)	2.58 (2.48-2.64)
CNR				
WM/GM	12.4 (8.6-15.7)	13.2 (10.4-17.7)	13.5 (9.0-18.4)	16.0 (11.8-22.1)
WM/CSF	19.2 (13.8-30.5)	33.7 (22.9-45.8)	3.1 (1.2-6.4)	27.4 (17.3-36.2)
GM/CSF	4.2 (1.9-7.0)	22.5 (14.2-29.5)	2.9 (1.1-5.9)	16.4 (10.0-22.8)
TotalCNR**	35.8 (25.5-52.0)	69.3 (49.2-87.6)	19.5 (12.7-30.8)	59.8 (39.2-79.0)

WM: White Matter, GM: Gray Matter, CSF: Cerebrospinal Fluid. CN and CNR measurements were performed in the corpus callosum (splenium) for WM, caudate nucleus (head) for GM and lateral ventricle for CSF. Ranges of *CN* and *CNR* are presented in parentheses.

*TotalCN is the mean sum of the contrast WM/GM, WM/CSF and GM/CSF calculated for each volunteer.

**TotalCNR is the mean sum of the contrast to noise ratios WM/GM, WM/CSF and GM/CSF calculated for each volunteer.

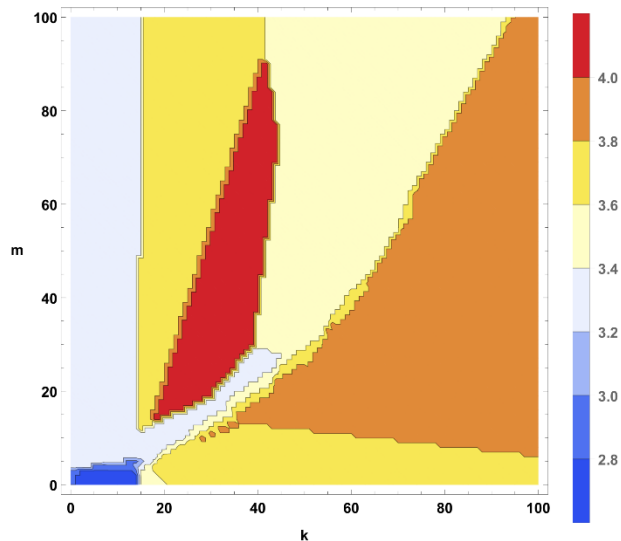


Figure 1: Sum of the simulated contrast between brain tissues for the pre-optimal parameter sets

$\Phi_{\text{opt}}^{k,m}$ according to the pair of regularization parameters (k,m) .

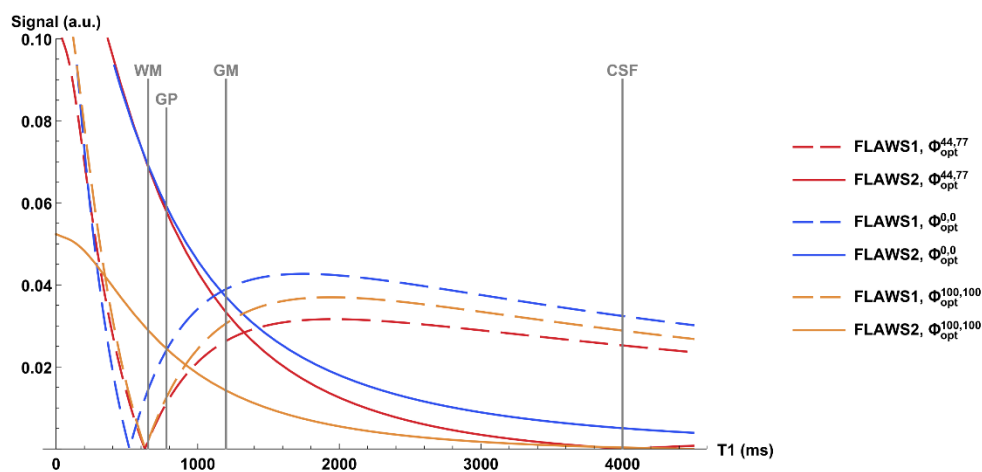


Figure 2: Signal simulation of *FLAWS1* and *FLAWS2* for the pre-optimal parameter sets $\Phi_{\text{opt}}^{k,m}$ corresponding to the pair of regularization parameters $(k = 44, m = 77)$, $(k = 0, m = 0)$ and $(k = 100, m = 100)$. WM: white matter; GP: globus pallidus; GM: gray matter; CSF: cerebrospinal fluid.

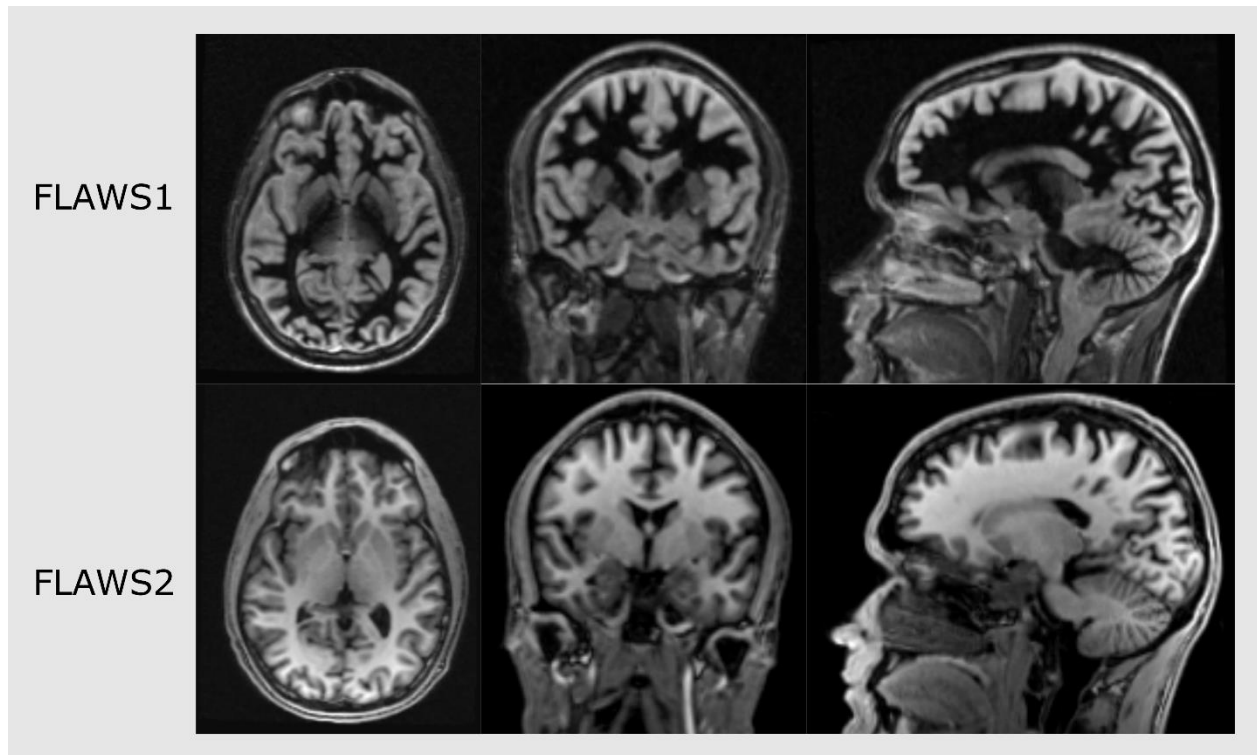


Figure 3: Axial (left), coronal (center) and sagittal (right) 1.5T FLAWS images acquired with the optimal set of parameters Φ_{opt} , presented in Table 1.

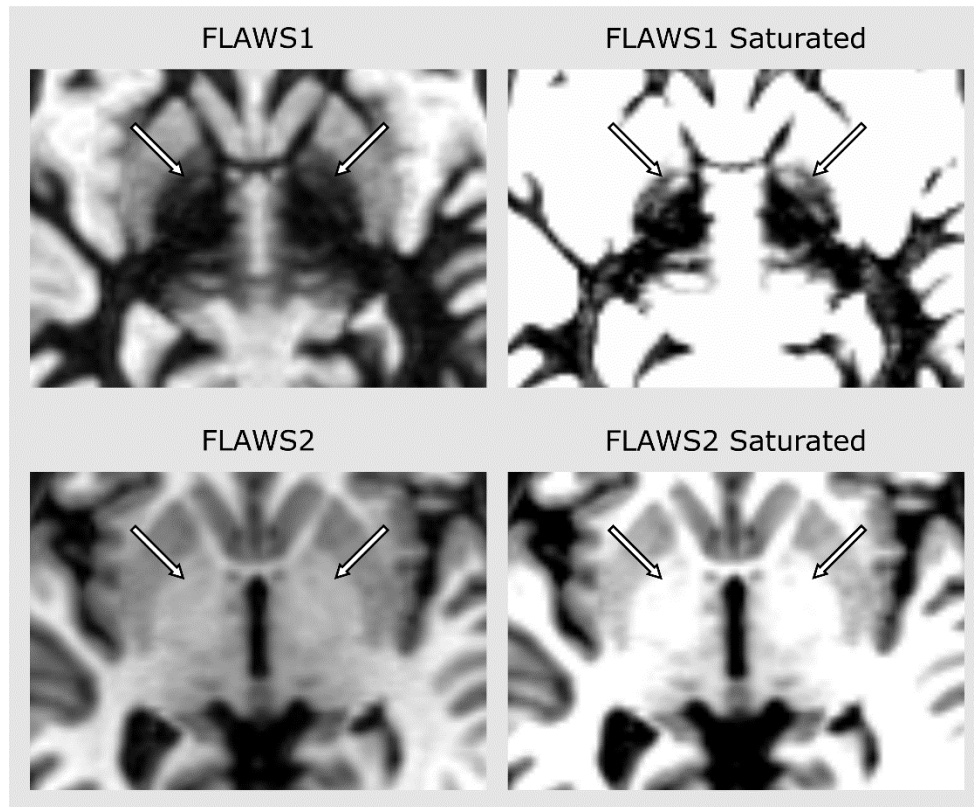


Figure 4: Visualization of the basal ganglia with FLAWS at 1.5T. The arrows indicate the location of the separation between the internal and the external globus pallidus. The identification of globus pallidus structures is easier in *FLAWS1* (first row) than in *FLAWS2* (second row). *FLAWS1* and *FLAWS2* images are also displayed with a saturated signal window to better visualize the separation between the internal and the external globus pallidus in the printed version of the paper.

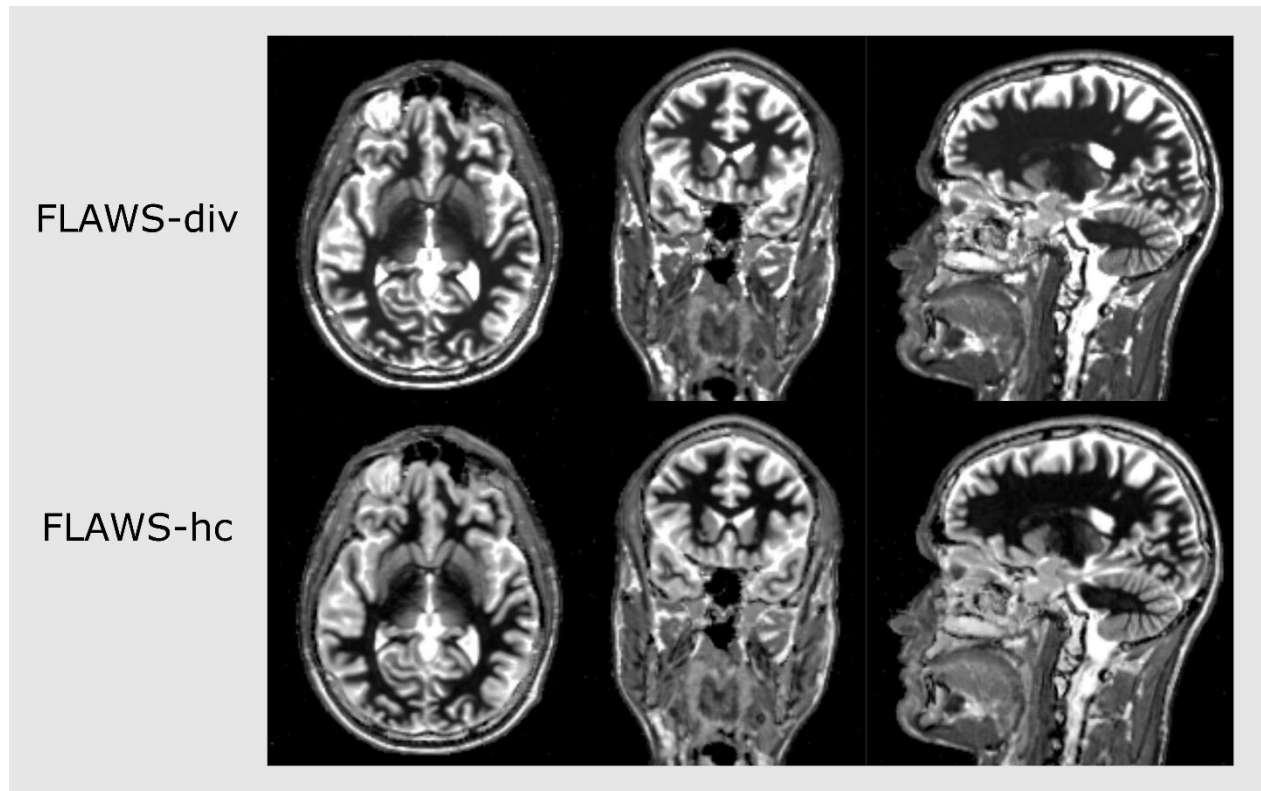


Figure 5: Axial (left), coronal (center) and sagittal (right) image combination *FLAWS-div* (first row) and *FLAWS-hc* (second row). These images were denoised by adding coefficients in the voxel-wise combinations [16].

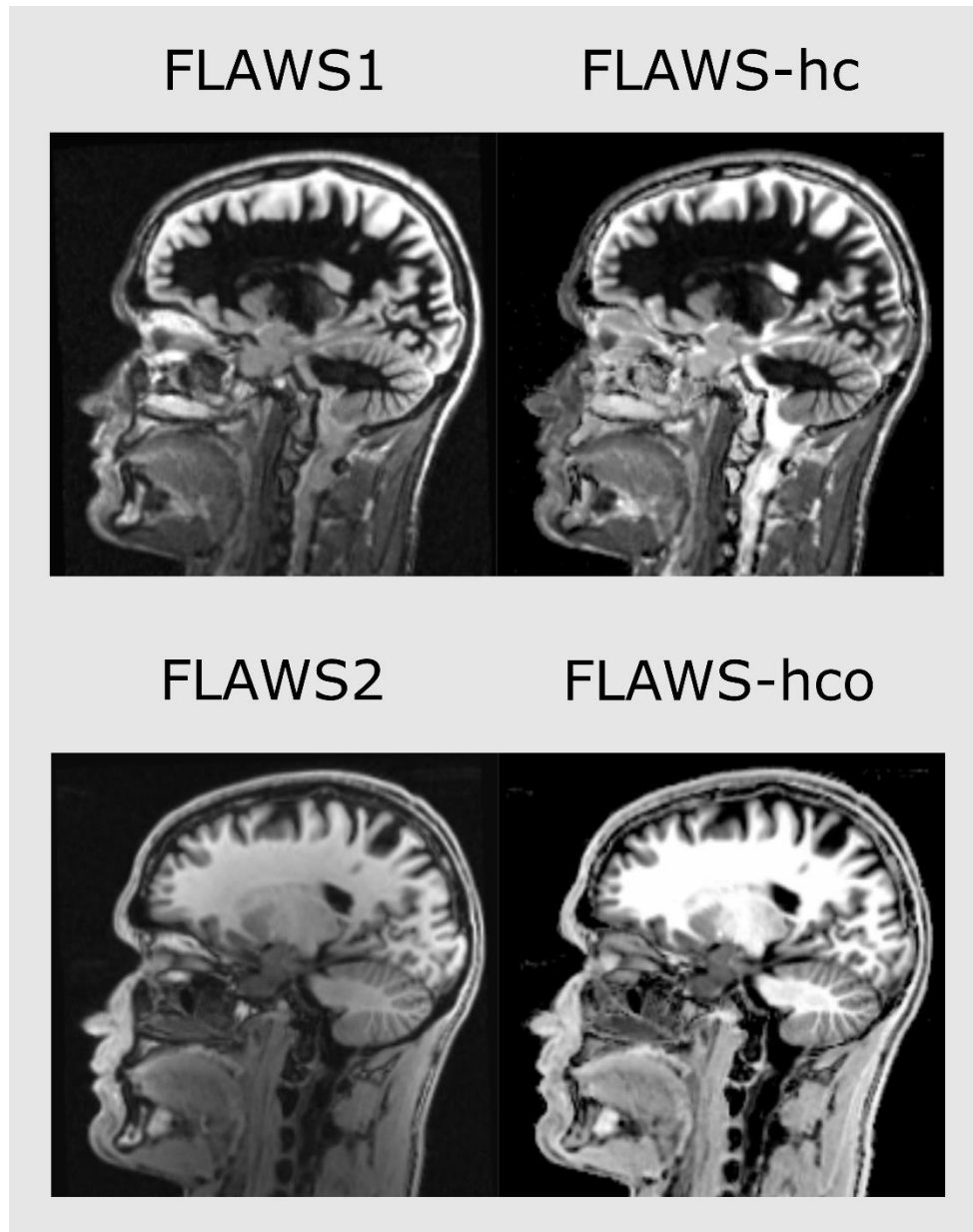


Figure 6: Sagittal views of *FLAWS1* and *FLAWS-hc* (first row) and *FLAWS2* and *FLAWS-hco*, the opposite of *FLAWS-hc* (second row).

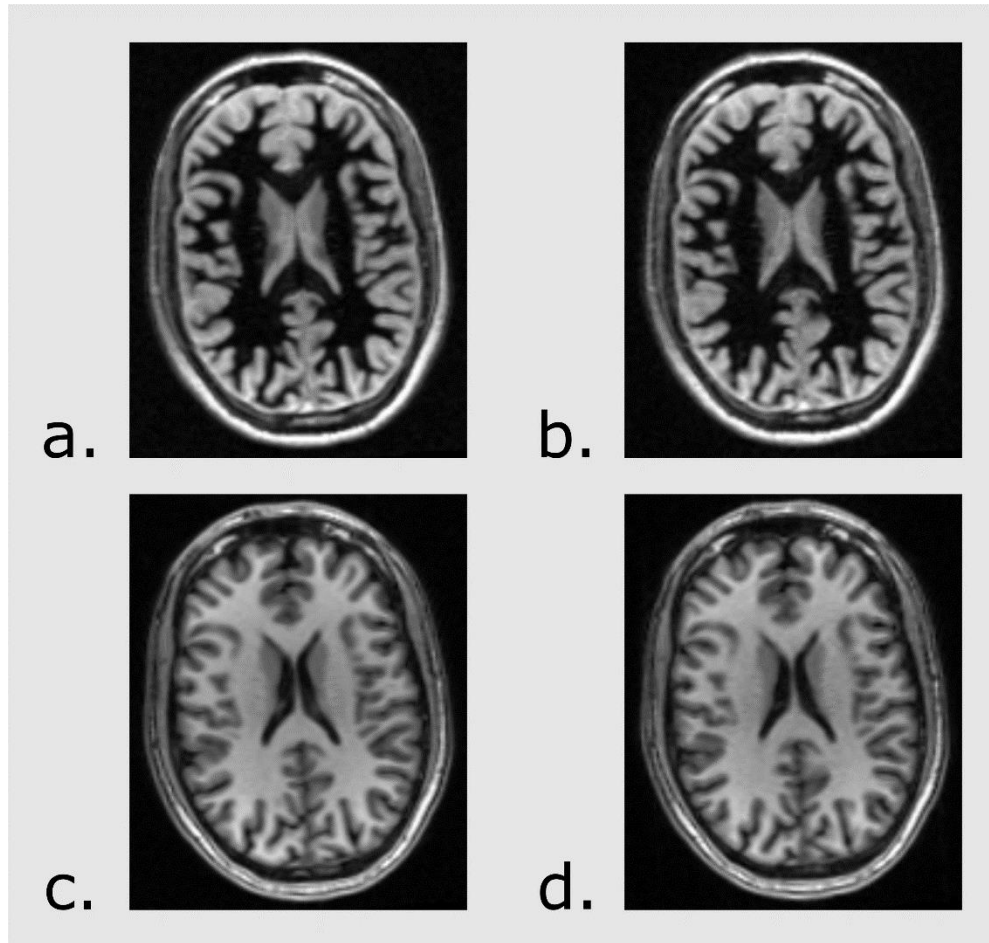


Figure 7: Examples of FLAWS1 (top row) and FLAWS2 (bottom row) images acquired at 1.5T without parallel imaging (a, c) and with parallel imaging (b, d).

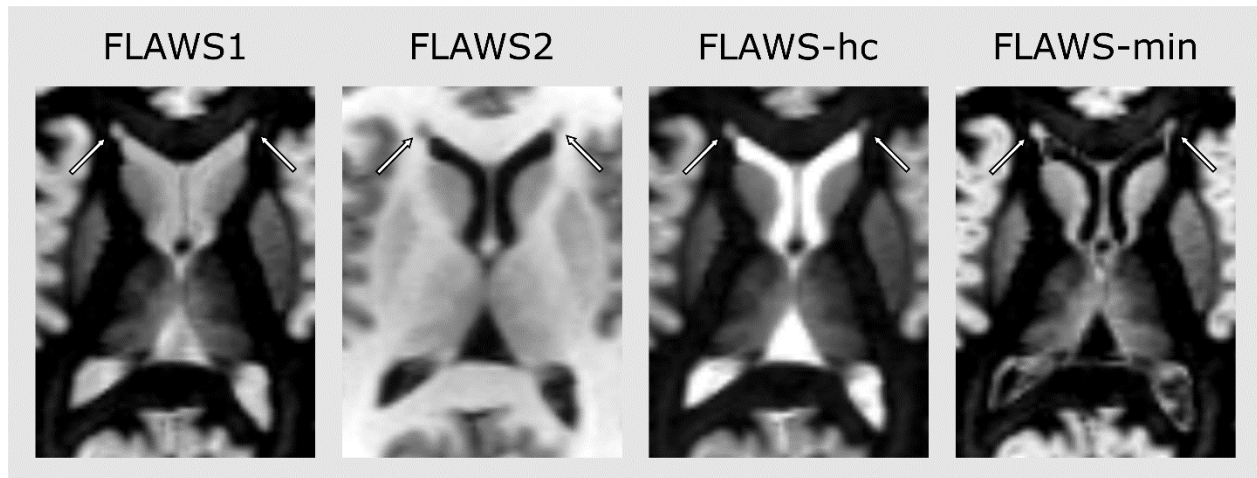


Figure 8: Axial FLAWS images showing an incidental finding (periventricular GM heterotopia) observed in one volunteer. The contrast enhancement provided by *FLAWS-hc* allows to better identify the incidental finding. This incidental finding was also clearly identified in the FLAWS minimum image (*FLAWS-min*).